Journal of Vacuum Science and Technology B

RESEARCH ARTICLE | OCTOBER 24 2024

# Twin-free thermal laser epitaxy of Si on sapphire

Thomas J. Smart ; Dong Yeong Kim ; Wolfgang Braun



*J. Vac. Sci. Technol. B* 42, 062204 (2024)
https://doi.org/10.1116/6.0003945

JVST B
Journal of Vacuum Science & Technology B

ARTICLE

pubs.aip.org/avs/jvb

# Twin-free thermal laser epitaxy of Si on sapphire

Cite as: J. Vac. Sci. Technol. B 42, 062204 (2024); doi: 10.1116/6.0003945
Submitted: 31 July 2024 · Accepted: 3 October 2024 ·
Published Online: 24 October 2024



Thomas J. Smart,[1] Dong Yeong Kim,[2,a)] and Wolfgang Braun[3]

## AFFILIATIONS

[1]Peter Grünberg Institut (PGI-9), Forschungszentrum Jülich, Jülich 52425, Germany
[2]Major of Semiconductor Engineering, Pukyong National University, 45 Yongso-ro, Nam-gu, Busan 48513, Republic of Korea
[3]epiray GmbH, Heinrich-Otto-Str. 73, Wendlingen 73240, Germany

[a)]**Author to whom correspondence should be addressed:** dykim@pknu.ac.kr

## ABSTRACT

The heteroepitaxial growth of silicon (Si) is essential for modern electronics. Our study investigates the potential of thermal laser epitaxy (TLE) for Si epitaxy. A systematic study on the evaporation behavior of Si during TLE identifies and addresses the causes of notable flux rate fluctuations, resulting in a Si flux with $\pm 0.3\%$ stability over time. We also demonstrate heteroepitaxy of Si on *c*-plane sapphire substrates via TLE. High-temperature substrate preparation combined with deposition at a substrate temperature of 1000 °C produced high-quality epitaxial Si (111) films without twin domains.





## I. INTRODUCTION

Modern electronic technology relies on Si and its semiconducting properties, with Si epitaxy being a key process for Si electronics. For instance, silicon-on-insulator (SOI) technology uses high-quality single crystalline Si films grown on insulating substrates, enhancing the performance of Si-based electronics and facilitating miniaturization. Sapphire ($Al_2O_3$) is an attractive insulator for SOI due to its outstanding properties such as excellent electrical insulation, high thermal stability, high mechanical strength, and high radiation resistance.[1–5] These properties make silicon-on-sapphire (SOS) an efficient platform for complementary metal-oxide-semiconductor (CMOS) technology.[6–8]

SOS epitaxy has been achieved by various vapor-phase epitaxy techniques, including chemical vapor deposition (CVD) and molecular beam epitaxy (MBE). In CVD, silane ($SiH_4$) is pyrolyzed on substrates.[9] MBE involves the sublimation or evaporation of solid or liquid Si through thermal heating or electron-beam evaporation. MBE is known to yield superior Si films on sapphire substrates due to effective strain relaxation.[10–12] However, CVD is the standard from a technological standpoint due to its higher productivity. Recently, a promising new physical vapor deposition technique has emerged called thermal laser epitaxy (TLE), wherein free-standing sources of material are locally heated by continuous-wave (CW) lasers.[13] This allows for the deposition of any solid, nonradioactive element from across the periodic table,[14] and the ability to deposit compounds via the use of a reactive atmosphere.[15–17] The localized heating induced by the laser beam allows the source to act as its own crucible, eliminating the need for a crucible made from a different material, while at the same time reducing the amount of required source material compared to other physical vapor deposition (PVD) techniques[14] and reduced deposition system size. With the addition of a $CO_2$ laser substrate heater, particularly for oxide substrates,[18,19] TLE has already been highly successful in the growth of epitaxial films.[20]

For the application of TLE to semiconductor electronics, flux stability is a key requirement for sample uniformity and reproducibility. This is particularly important for selective growth using stencil masks and precisely defined layers to produce a device.[21] Achieving stable deposition of Si proves challenging for most PVD techniques utilizing vaporization, due to the highly reactive nature of Si with common crucible materials.[22–25]

In this study, we investigate the potential of Si epitaxy using TLE, with a specific focus on achieving flux scalability and control. A reproducible Si flux with a standard deviation of $\pm 0.3\%$ is achieved by identifying and addressing sources of flux fluctuations in TLE, namely, source deformation and the coating of optics. We also demonstrate Si heteroepitaxy on *c*-plane sapphire substrates. We discuss the growth of amorphous, polycrystalline, and epitaxial Si films on *c*-plane sapphire substrates, as well as the complete desorption of Si entailing sapphire etching, over a wide range

of substrate temperatures $T_S$ from 20 to over 1200 °C. High-temperature substrate preparation and film growth results in twin-free Si (111) films on *c*-plane sapphire substrates.

## II. EXPERIMENT

Pure (99.999%) cylindrical sources of Si are thermally evaporated inside a TLE chamber using laser radiation as shown in Fig. 1. The Si source has a diameter of 12 mm and a height of 8 mm. Localized laser heating of the sources is provided by a CW laser beam with a wavelength of 515 or 1030 nm, both with a laser spot size of approximately 1 $mm^2$. The laser beam has a Gaussian intensity profile and impinges at an angle of 45° on the upper circular face of the Si source. Whereas the reflectivity and absorption coefficient of Si at these wavelengths affect the laser power $P$ required for evaporation, we find the physical behavior of Si during evaporation to be independent of the wavelength used. Within the deposition chamber, a mirror reflects the laser beam onto the Si source to prevent Si deposition on the laser entrance window of the deposition chamber at the expense of Si deposition on the mirror. Such a mirror enhances the uptime of the laser optics because Si coating affects the reflectance of a mirror less than the transmission of a window.[26] This mirror-based system is common to current TLE systems.

Linear motors on the system drive the manipulator arm on which the Si source is placed in orthogonal horizontal directions. This allows for a relative motion of source and laser beam with a fixed position of the laser beam on the source with respect to the substrate. Thereby, the source moves underneath the laser spot where evaporation takes place. In particular, a circular motion of radius $r$ can be implemented.

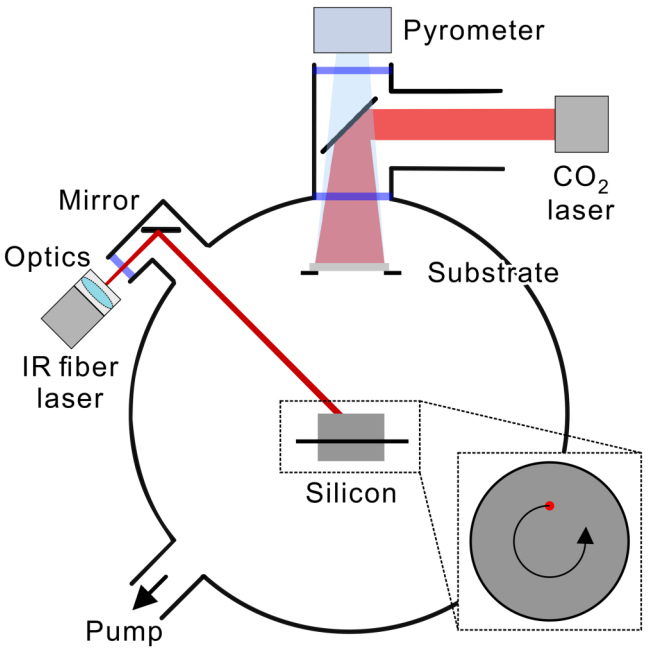


**FIG. 1.** Cross-sectional sketch of the TLE chamber used for growing Si films. The inset shows the relative motion of the incident laser beam to the Si source.

For deposition, a 10 × 10 mm *c*-plane sapphire substrate is positioned 60 mm above the Si source. The substrate's backside is heated to the required process temperature using a $CO_2$ laser with a wavelength of 10.6 μm.[19] The substrate laser beam has an intensity profile tailored to produce a uniform temperature across the substrate's backside, which is monitored on-axis via a beam splitter with a calibrated pyrometer. The calibration factor of the pyrometer is determined by the ratio of the measured temperature to the melting temperature of the sapphire substrate (2040 °C). Melting on the back of substrates is observable through the transparent substrate by a camera mounted on the chamber facing the front side of the substrate. The chamber's base pressure is maintained at $\leq 10^{-8}$ hPa, and the residual pressure during operation is kept at $<10^{-7}$ hPa. The process chamber is water-cooled to 20 °C.

## III. RESULTS AND DISCUSSION

### A. Laser evaporation of Si

When irradiated by a sufficiently high laser power $P$, Si develops a localized liquid phase underneath the laser spot, as shown in the inset of Fig. 2(a). This liquid phase acts as an effective evaporation source, with the surrounding solid phase serving as a crucible for the liquid. This is consistent with the observation that localized laser heating can be used for crucible-free growth.[14]

The growth rate $\Gamma$ in TLE scales with $P$ as demonstrated in a previous study.[14,27] Empirically, as shown in Fig. 2, we find that the $\Gamma$ value of Si follows an Arrhenius-like dependence on $P$,

$$\Gamma = ae^{-\frac{b}{P}}, \quad (1)$$

where $a$ and $b$ are constants that may be determined from fitting this function to experimental data. In the case of a Si source with a source diameter of 12 mm, we obtain values of $a$ = 7.162 Å/s and $b$ = 1216 W.[27] In our experiment, $\Gamma$ is measured by a quartz crystal microbalance (QCM), with a tooling factor calibrated using cross-sectional scanning electron microscopy of cleaved samples. The observed Arrhenius-like dependence serves as a guide to predict $\Gamma$ of the source material at different values of $P$.

This Arrhenius-like dependence of $\Gamma$ persists over more than 2 orders of magnitude produced by the range of $P$ values explored within this work. In a previous study, it was found that $\Gamma$ of Al shows the Arrhenius-like behavior over more than 7 orders of magnitude up to the highest measured growth rate of ~3600 Å/s.[17,16] We, therefore, expect that this Arrhenius-like behavior for Si may hold over a larger range of laser power densities than those explored in this study. The parameters entering the Arrhenius-like dependence are influenced by the size of the source. With large sources, for example, high $\Gamma$ values are achievable, suitable for a 300-mm-wafer manufacturing process.[27] Figure 2(b) illustrates the measured correlation between $P$ and melt pool diameter $D$, which follows a linear dependence. Therefore, $D$ and $\Gamma$ are logarithmically related, as shown in Fig. 2(c). From this, a Si source with a 19-mm melt pool diameter is expected to be suitable to achieve a $\Gamma$ value of 1 Å/s for a 300 mm diameter wafer.

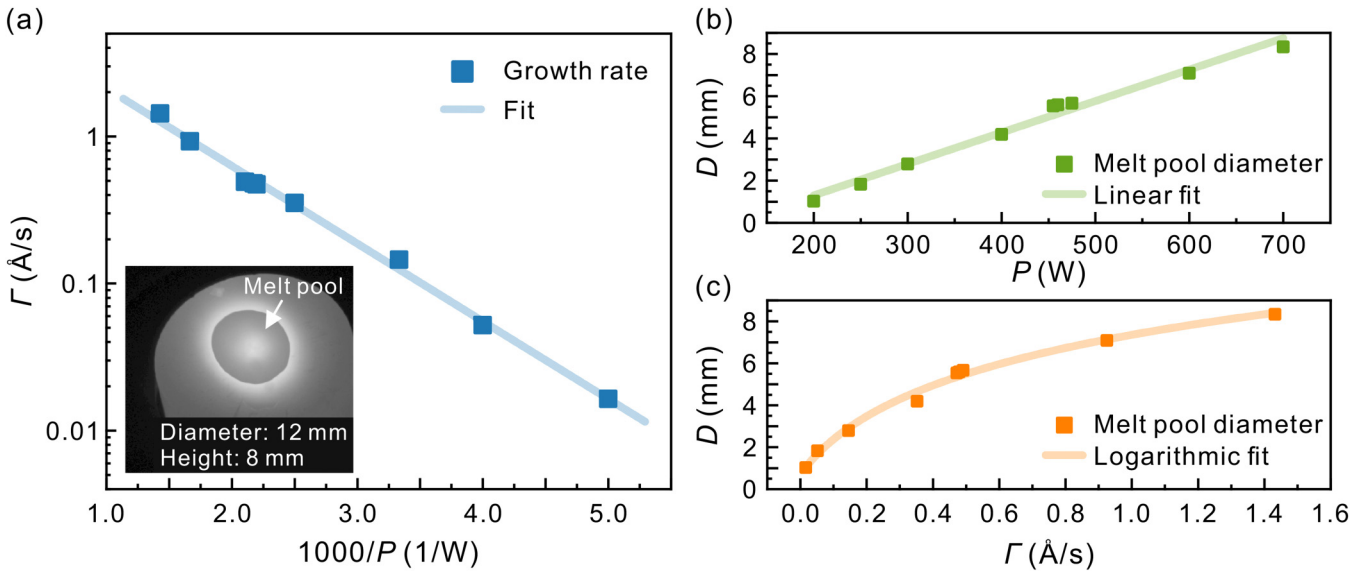


**FIG. 2.** (a) Growth rate $\Gamma$ of Si as a function of laser output power $P$. Data are taken from Ref. 27. The light blue line represents the Arrhenius-like fit of $\Gamma$ as a function of $P$ as given in Eq. (1). Orders of magnitude in growth rate are accessible within the dynamic range of the laser. (Inset) Image of a Si source during thermal laser evaporation, reproduced from Ref. 27. Reprinted with permission from T. J. Smart, "Thermal laser epitaxy: From fundamental physics to the growth of novel thin films," Ph.D. thesis (University of Stuttgart, 2023). A liquid melt pool is well visible around the laser beam. This laser beam has a size of $\simeq$1 mm$^2$. (b) Si melt pool diameter $D$ as a function of output laser power $P$. The light green line represents a linear fit. (c) Relationship between Si melt pool diameter $D$ and growth rate $\Gamma$ of Si. The light orange line is a logarithmic fit.

### B. Si flux stability

A key aspect in the growth of epitaxial high-quality films is a stable growth rate, ensuring growth reproducibility. In laser-based deposition, any optics within the line-of-sight of the evaporating source becomes coated with repeated deposition. This has been identified as one of the primary sources of unstable growth rates over time for laser-based deposition.[26]

We have identified two mechanisms during our experiments. The first mechanism is the changing morphology of the surface of the evaporating source during deposition. The second mechanism is the coating of the laser mirror during deposition.

Evaporation of the source mainly occurs at the location of the laser spot and depletes material within the melt pool, which subsequently forms a concave surface. This curvature distorts the ideal cosine flux distribution from flat surfaces and, therefore, the deposition rate of evaporating material arriving at the substrate.[28] In the extreme case of a highly focused laser spot with power density (>10$^6$ W/cm$^2$), recoil pressure from the evaporating material forms a deep and narrow depression within the material, as is the case for laser welding processes.[29] Within TLE, the curvature of the surface can be mitigated by increasing the size of the melt pool, either by increasing the size of the laser spot or by introducing relative motion between the source and the laser spot.

This relative motion effectively increases the size of the melt pool and reduces the local curvature of the melt pool caused by the pinning at its rim. A circular motion of the laser beam, as illustrated in Fig. 1, moves the liquid phase around the surface to cover a large area. This causes a flatter melt pool, thereby ensuring greater flux stability over time. Flux fluctuations due to the curved Si melt become repeatedly averaged per cycle such that stable evaporation is achieved on time scales longer than the cycling period.

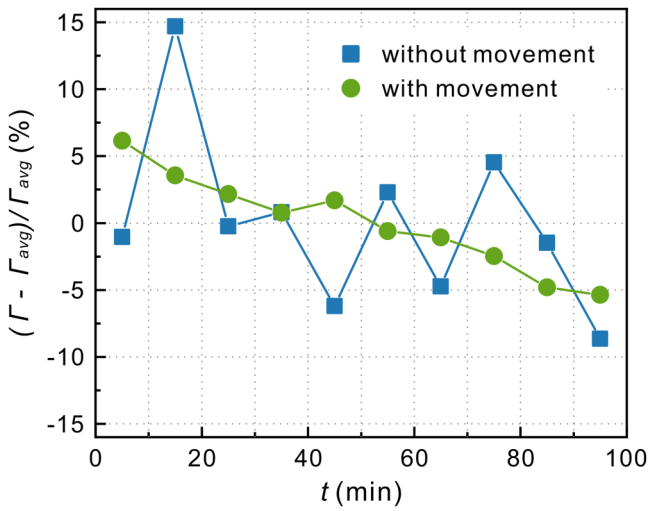


**FIG. 3.** Deviation in growth rates $\Gamma$ of Si from its time-averaged rate $\Gamma_{avg}$ as a function of time $t$ under constant laser power for both stationary and moving Si sources. Data are taken from Ref. 27.

With an appropriately shaped beam, a circular beam spot on the source surface may be achieved. In this configuration, with a circular motion at a constant angular speed, the source operates in a steady state in which the thermal distribution within the source is constant in a reference frame rotating with the circular motion. This allows highly stable evaporation or sublimation with a beam significantly smaller than the source diameter, allowing for a more efficient use of source material, while still being able to use a large area source for long campaign times.

To understand the effect that the continuous movement of the laser spot has upon the Si flux, we compare the deviation of $\Gamma$ from its time-averaged rate between a stationary source and a source moved along a circle with a radius of 1.5 mm. This is illustrated in Fig. 3, where the $P$ value is kept at 600 and 510 W, respectively. The Si flux varies by 5%–10% when Si is evaporated in the stationary case. This scatter is mainly caused by the fluctuating flux distribution due to the temporally changing surface orientation of the molten Si.

With continuous circular motion, the effect of source deformation is reduced and a gradually decreasing flux over time is measured. This we attribute to the second mechanism for flux instability in TLE: coating of the laser mirror, in this case, coating of the mirror with Si. Since the coating has a higher absorption than the original mirror surface, a larger fraction of the laser power is absorbed at the mirror surface, leading to a corresponding decay of the laser beam power arriving at the source.

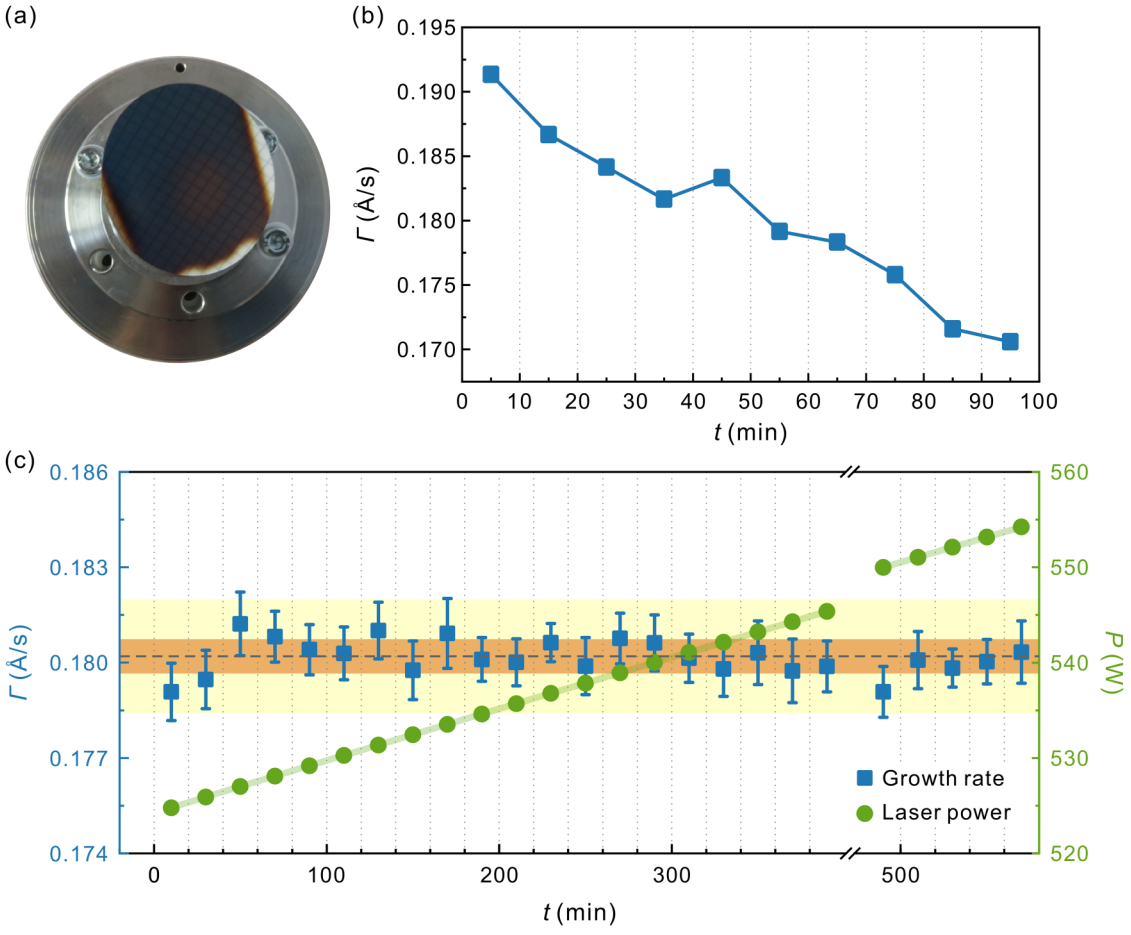


**FIG. 4.** (a) Photograph of a vacuum mirror and its coating after approximately three months of operation, reproduced from Ref. 27. Reprinted with permission from T. J. Smart, "Thermal laser epitaxy: From fundamental physics to the growth of novel thin films," Ph.D. thesis (University of Stuttgart, 2023). (b) Growth rate $\Gamma$ of Si as a function of time for $P$ = 510 W and $\lambda$ = 515 nm. The relative position of the laser spot upon the source was continuously moved on a circular path with a radius of 1.5 mm as described previously. (c) Growth rate $\Gamma$ of Si for repeated 20 min-long depositions. The output laser power is shown on the second axis. The orange and yellow bands represent the $\pm$0.3 % and the $\pm$1 % range of the averaged growth rate of Si, respectively. The error bars of the growth rate measurements mainly represent uncertainties from the temperature sensitivity of the QCM. The gap in the data represents a period of time where Si was not deposited inside the chamber, after which a new Si source was placed inside and deposition continued. The average growth rate (dashed line) is 0.1802 $\pm$ 0.0005 Å/s (standard deviation). Data within this figure are taken from Ref. 27.

The laser mirror is located directly in the line of sight of the source in the TLE chamber. Consequently, the source material deposits along the same line of sight onto the laser mirror during the evaporation process. The mirror surface gradually changes from its original material to Si, with associated changes in reflectivity. Figure 4(a) shows a photograph of a mirror after approximately three months of continuous operation. It is covered by a significant coating that reduces its reflectivity. Nevertheless, the accurately reflected grid pattern of the cleanroom suit indicates negligible roughening associated with this cover layer.

Figure 4(b) displays the $\Gamma$ value delivered by one Si source over a sequence of depositions using a laser power of 510 W and circular motion with a radius of 1.5 mm. This figure is based on the measurement data shown as circular dots in Fig. 3. The data show a clear monotonic decrease of $\Gamma$ as a function of time, which is attributed to a reduction in the incident laser power upon the source caused by coating of the laser mirror with evaporated source material. Independent of its origin, this effect can empirically be compensated by increasing $P$ with time. The coating of the mirror with time also explains the difference between the recorded $\Gamma$ in Fig. 4(b) at $P$ = 510 W and the expected growth rate of ~0.7 Å/s at $P$ = 510 W extrapolated from the Arrhenius-like dependence for $\Gamma$ as a function of $P$ shown in Fig. 2. Coating of the laser mirror reduces the incident laser power upon the source $P_{in}$ and thus changes $\Gamma$.[26] Hence, the output laser power $P$ must be continuously adapted to account for the decreasing reflectivity of the mirror.

Using the Arrhenius-like $\Gamma$ dependence as a function of $P$ as previously shown in Fig. 2, we can estimate the incident laser power $P_{in}$ from $\Gamma$. The reflectance of the mirror can then be calculated by using the ratio between the estimated value of $P_{in}$ and the nominal laser power $P$ of 510 W. To do so, we fit the time-dependent reflectance of the mirror $R_{mirr}(t)$ to a simple linear decay model,

$$R_{mirr}(t) = R_0 - \beta t, \tag{2}$$

where $R_0$ is the initial reflectance of the laser mirror before coating and $\beta$ is the rate of decay of the mirror reflectance per time $t$ of operation.

From $R_{mirr}(t)$, we derive the value of $P(t)$ required to maintain a constant $P_{in}$,

$$P(t) = \frac{P_{in}}{R_{mirr}(t)}. \tag{3}$$

Laser power compensation according to Eq. (3), along with the relative motion of Si source and laser beam, lead to a stable growth rate as a function of time [Fig. 4(c)]. Note that in our

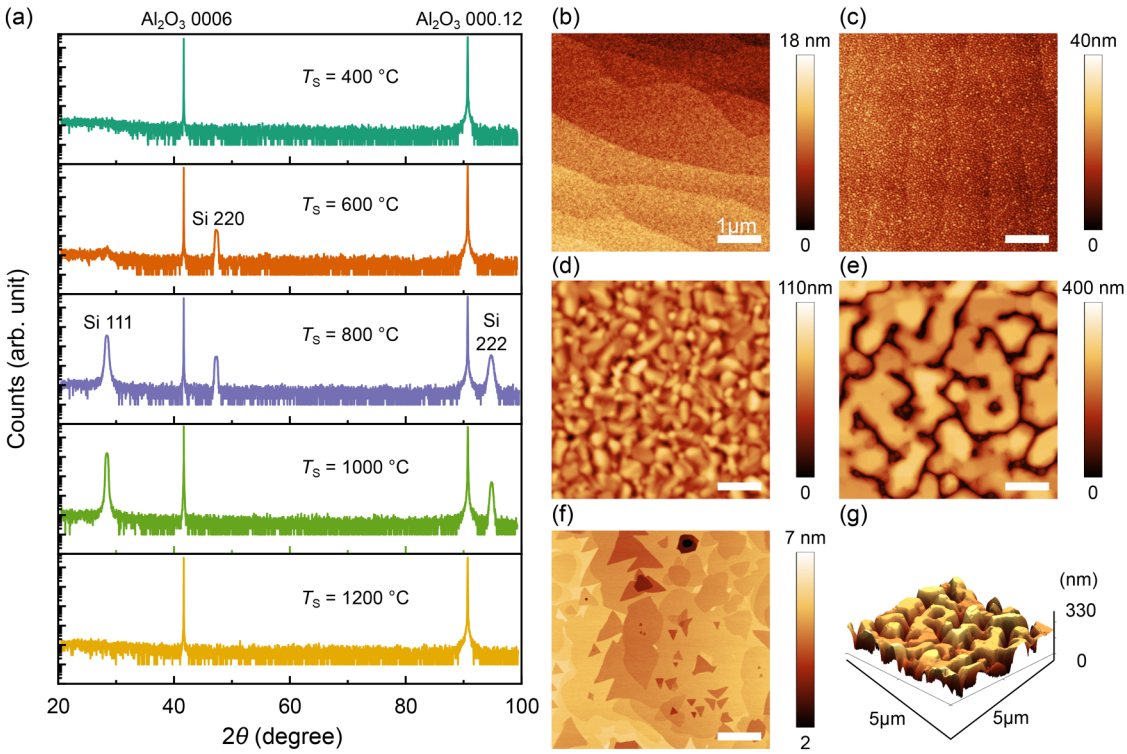


**FIG. 5.** (a) XRD 2$\theta$-$\omega$ patterns of Si films grown on *c*-plane sapphire substrates at several substrate temperatures from 400 to 1200 °C. AFM images of the surface morphology of the Si films on *c*-plane sapphire substrates grown at (b) 400, (c) 600, (d) 800, (e) 1000, and (f) 1200 °C. The lateral scale bars in the AFM images are 1 μm long. (g) Three-dimensional AFM profile of Si film grown at 1000 °C.

experiments, the source was moved relative to a fixed laser beam, resulting in a stationary position of the evaporation area with respect to the substrate. In a situation with coevaporation from several sources, it may be advantageous to move the laser beams with fixed source positions, instead. This should not significantly affect the deposition stability, as long as the radius of the relative circular motion, and therefore the movement of the evaporation area with respect to the substrate, is small compared to the substrate size.

The error bars observed for each data point in Fig. 4(c) result from temperature instabilities in the cooling circuit of the QCM used to measure the growth rate, which remained consistent between data points. For the entire set of experiments, a growth rate $\Gamma = 0.1802 \pm 0.0005$ Å/s (standard deviation) was obtained, corresponding to a $\pm 0.3\%$ deviation. This standard deviation value is comparable to, or below, the typical value of $\pm 1\%$ for effusion cells used in molecular beam epitaxy.[30] This result is further compounded by the fact that Si strongly reacts with many common crucible materials used in effusion cells, making the achievement of high and stable Si fluxes above its melting point challenging.[22,23,25,31]

The gap in the data of Fig. 4(c) indicates an 80-min deposition time period during which the Si source was replaced with a new one, and some initial calibration measurements were performed outside the current work. We resumed the experiments using the fresh Si source by extrapolating the exponential dependence of the output laser power. The results, shown in Fig. 4(c), confirm that the results are not limited to a single source, rather stability in the Si flux can be perpetuated by following the prior algorithm, resulting in the previously measured growth rate.

### C. Si heteroepitaxy on *c*-plane sapphire substrates

The prior investigation of Si flux stability in TLE was then applied to the heteroepitaxial growth of Si on *c*-plane sapphire substrates at various substrate temperatures $T_S$. Prior to Si evaporation, the substrates were thermally prepared *in situ* by heating them to 1800 °C for 5 min under ultrahigh vacuum conditions within the TLE chamber. This step is crucial for epitaxy because it cleans the surface by evaporating any volatile contaminants, induces sufficient surface mobility to form the lowest energy surface-step-and-terrace system, and results in a $(\sqrt{31} \times \sqrt{31})$ $R + 9°$ or $R - 9°$ double-stepped surface reconstruction.[18] This high-temperature preparation step is essential for the growth of twin-free (111) Si films on *c*-plane sapphire substrates, as will be discussed below.

Figure 5(a) shows the X-ray diffraction (XRD) $2\theta$-$\omega$ patterns of Si films grown at various $T_S$ ranging from 400 to 1200 °C. When the films are grown at 400 °C, the Si films are amorphous, and the surface morphology appears flat, following the terraces of the underlying substrate [Fig. 5(b)]. As $T_S$ increases, crystalline Si films begin to form, and the Si (110) crystal orientation dominates in films grown at 600 °C. At both 400 and 600 °C, granular structures are observed in AFM, but the terrace structure of the substrate is still discernible (Fig. 5(c)). The Si films grown at 800 °C show both Si 111 and Si 220 reflections, whereas the X-ray scans of the 1000 °C films only measure the Si 111 reflection. Starting at 800 °C, the surface morphology also changes [Figs. 5(d) and 5(e)]. The grain size increases, eventually leading to large mesa islands at 1000 °C with flat and smooth top surfaces, but separated by deep trenches, likely down to the substrate surface. A three-dimensional rendering of the surface of the Si film grown at 1000 °C is presented in Fig. 5(g).

We observe a significant decrease in the growth rate as $T_S$ increases from 800 to 1000 °C caused by the desorption of Si from the substrate. Such growth conditions with sticking factors of <1 yield films of higher purity. Impurities with a lower binding energy than Si have a lower probability of being incorporated into the lattice of the growing film. These would then preferentially desorb under such near-equilibrium conditions. By increasing $T_S$ further to >1200 °C, we find that Si likely reacts with the sapphire substrate, consuming oxygen from it and forming volatile $Al_2O$ and SiO ($2Si + Al_2O_3 \longrightarrow 2SiO + Al_2O$),[32] resulting in characteristic monolayer triangular etch pits on the surface as shown in Fig. 5(f).

The epitaxial growth of Si (111) film at 1000 °C is confirmed by XRD $\phi$ scans of Si 220 and $Al_2O_3$ 104 Bragg reflections, as shown in Fig. 6(a). The (111) plane of the diamond cubic structure exhibits threefold symmetry, matching the observed three peaks separated by 120° in XRD $\phi$ scans of the Si 220 reflections. This confirms, within the detection limit, the absence of twinned domains in TLE-grown Si films on *c*-plane sapphire substrates. Twin-free Si (111) growth was also confirmed via electron

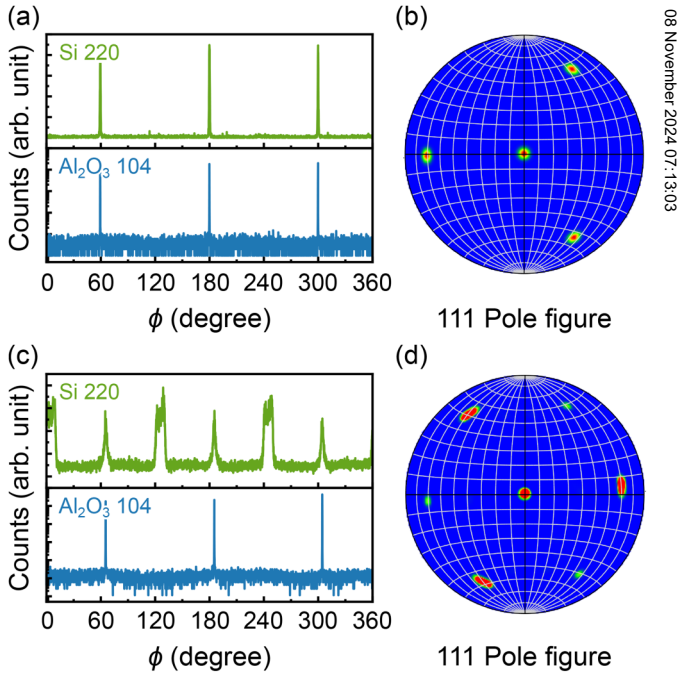




**FIG. 6.** (a) XRD $\phi$ scans of Si 220 and $Al_2O_3$ 104 Bragg reflections and (b) 111 pole figure derived from EBSD analysis of Si films grown after high-temperature sapphire preparation at 1800 °C for 5 min in vacuum. (c) XRD $\phi$ scans of Si 220 and $Al_2O_3$ 104 Bragg reflections and (d) 111 pole figure of Si films grown on bare *c*-plane sapphire substrates.

backscatter diffraction (EBSD) analysis. The 111 pole figure of the epitaxial Si film closely resembles the standard 111 pole figure of a (111) cubic single crystal [Fig. 6(b)].

We find that the high-temperature substrate preparation is a key process for growing twin-free Si (111) epitaxial films on *c*-plane sapphire substrates. Further refinement of the high-temperature annealing process of sapphire promises the formation of twin-free Si films irrespective of film thickness. This remains the subject of future study. On bare substrates that were just heated to the process temperature of 1000 °C, Si films grow epitaxially but are twinned [Figs. 6(c) and 6(d)]. In such films, the twinned domain dominates, even showing split diffraction peaks, indicating that the twin domain consists of multiple subdomains.

## IV. CONCLUSIONS

We have demonstrated the heteroepitaxy of Si thin films on *c*-plane sapphire substrates using TLE. By adopting a relative motion between the incoming laser beam and the source and by compensating for laser power attenuation at the mirror, we have achieved a Si flux that is highly stable over many hours of deposition time across 25 growths with a standard deviation of $\pm 0.3\%$. By increasing the substrate temperature during film growth from 400 to 1200 °C, amorphous, polycrystalline, and epitaxial growth as well as complete desorption were observed. The *in situ* high-temperature substrate preparation and high-temperature growth used in TLE lead to the reliable growth of Si (111) films on *c*-plane sapphire substrates. These results demonstrate the potential of TLE for Si and SOS technologies.

## ACKNOWLEDGMENTS

The authors thank Abdur Rehmen Jalil, Peter Schüffelgen, Hans Boschker, Sander Smink, and Jochen Mannhart for insightful discussions and Bernhard Fenk for the EBSD measurements. The authors are grateful to Fabian Felden, Ingo Hagel, Konrad Lazarus, Sabine Seiffert, and Wolfgang Winter for technical support.

## AUTHOR DECLARATIONS

### Conflict of Interest

The authors have no conflicts to disclose.

### Author Contributions

Thomas J. Smart and Dong Yeong contributed equally to this paper.

**Thomas J. Smart:** Conceptualization (equal); Data curation (lead); Formal analysis (supporting); Validation (lead); Visualization (supporting); Writing – original draft (equal); Writing – review & editing (supporting). **Dong Yeong Kim:** Conceptualization (equal); Data curation (supporting); Formal analysis (lead); Visualization (lead); Writing – original draft (equal); Writing – review & editing (equal). **Wolfgang Braun:** Conceptualization (supporting); Data curation (supporting); Formal analysis (supporting); Supervision (lead); Writing – original draft (supporting); Writing – review & editing (equal).

## DATA AVAILABILITY

The data that support the findings of this study are available from the corresponding author upon reasonable request.

## REFERENCES

[1]P. D. Lomer, Proc. Phys. Soc., Sect. B **63**, 818 (1950).
[2]W. H. Rippard, A. C. Perrella, F. J. Albert, and R. A. Buhrman, Phys. Rev. Lett. **88**, 046805 (2002).
[3]V. Edlmayr, M. Moser, C. Walter, and C. Mitterer, Surf. Coat. Technol. **204**, 1576 (2010).
[4]V. N. Kurlov, in *Encyclopedia of Materials: Science and Technology*, edited by K. J. Buschow, R. W. Cahn, M. C. Flemings, B. Ilschner, E. J. Kramer, S. Mahajan, and P. Veyssière (Elsevier, Oxford, 2001), pp. 8259–8264.
[5]G.-G. Wang, J.-C. Han, H.-Y. Zhang, M.-F. Zhang, H.-B. Zuo, Z.-H. Hu, and X.-D. He, Cryst. Res. Technol. **44**, 995 (2009).
[6]C. Mueller and P. Robinson, Proc. IEEE **52**, 1487 (1964).
[7]R. Johnson, P. de la Houssaye, C. Chang, P.-F. Chen, M. Wood, G. Garcia, I. Lagnado, and P. Asbeck, IEEE Trans. Electron Devices **45**, 1047 (1998).
[8]D. Kelly, C. Brindle, C. Kemerling, and M. Stuber, "The state-of-the-art of silicon-on-sapphire CMOS RF switches," in *IEEE Compound Semiconductor Integrated Circuit Symposium, 2005 (CSIC'05)*, Palm Springs, CA, 30 October–2 November 2005 (IEEE, 2005), p. 4.
[9]J. Amano and K. W. Carey, J. Cryst. Growth **56**, 296 (1982).
[10]M. E. Twigg, E. D. Richmond, and J. G. Pellegrino, Appl. Phys. Lett. **54**, 1766 (1989).
[11]E. D. Richmond, M. E. Twigg, S. Qadri, J. G. Pellegrino, and M. T. Duffey, Appl. Phys. Lett. **56**, 2551 (1990).
[12]E. D. Richmond, J. G. Pellegrino, M. E. Twigg, S. Qadri, and M. T. Duffy, Thin Solid Films **192**, 287 (1990).
[13]W. Braun and J. Mannhart, AIP Adv. **9**, 085310 (2019).
[14]T. J. Smart, J. Mannhart, and W. Braun, J. Laser Appl. **33**, 022008 (2021).
[15]D. Y. Kim, J. Mannhart, and W. Braun, APL Mater. **9**, 081105 (2021).
[16]T. J. Smart *et al.*, J. Vac. Sci. Technol. A **41**, 042701 (2023).
[17]D. Y. Kim, T. J. Smart, L. Majer, S. Smink, J. Mannhart, and W. Braun, J. Appl. Phys. **132**, 245110 (2022).
[18]S. Smink, L. N. Majer, H. Boschker, J. Mannhart, and W. Braun, Adv. Mater. **36**, 2312899 (2024).
[19]W. Braun, M. Jäger, G. Laskin, P. Ngabonziza, W. Voesch, P. Wittlich, and J. Mannhart, APL Mater. **8**, 071112 (2020).
[20]D. Y. Kim, J. Mannhart, and W. Braun, J. Vac. Sci. Technol. A **39**, 053406 (2021).
[21]P. Schüffelgen *et al.*, Nat. Nanotechnol. **14**, 825 (2019).
[22]S. P. Murarka and D. B. Fraser, J. Appl. Phys. **51**, 1593 (1980).
[23]A. Christou and H. M. Day, J. Electron. Mater. **5**, 1 (1976).
[24]A. Maity, H. Das, D. Kalita, N. Kayal, T. Goswami, and O. Chakrabarti, J. Eur. Ceram. Soc. **34**, 3499 (2014).
[25]M. P. Siegal, W. R. Graham, and J. J. Santiago, J. Appl. Phys. **66**, 6073 (1989).
[26]J. T. Cheung and H. Sankur, Crit. Rev. Solid State Mater. Sci. **15**, 63 (1988).
[27]T. J. Smart, "Thermal laser epitaxy: From fundamental physics to the growth of novel thin films," Ph.D. thesis (University of Stuttgart, 2023).
[28]M. Knudsen, *The Kinetic Theory of Gases: Some Modern Aspects*, Methuen's Monographs on Physical Subjects (Methuen and Co. Ltd., London, 1952)
[29]J. Y. Lee, S. H. Ko, D. F. Farson, and C. D. Yoo, J. Phys. D: Appl. Phys. **35**, 1570 (2002).
[30]J. N. Eckstein, I. Bozovic, M. E. Klausmeier-Brown, G. F. Virshup, and K. S. Rails, MRS Bull. **17**, 27 (1992).
[31]J. Grabmaier, *Silicon Chemical Etching* (Springer, Berlin, 1982).
[32]H. M. Manasevit and W. I. Simpson, J. Appl. Phys. **35**, 1349 (1964).